Journal of Power Sources 196 (2011) 2075–2079

Contents lists available at ScienceDirect

Journal of Power Sources

journal homepage: www.elsevier.com/locate/jpowsour

Short communication

Stable and easily sintered $(Pr_{0.5}Nd_{0.5})_{0.7}Ca_{0.3}CrO_{3-\delta}/Sm_{0.2}Ce_{0.8}O_{1.9}$ composite interconnect materials for IT-solid oxide fuel cells

Yanzhi Ding[a,b], Xiaoyong Lu[b], Yonghong Chen[b], Bin Lin[b], Xingqin Liu[a,*], Guangyao Meng[a]

[a] CAS Key Laboratory of Materials for Energy Conversion and Laboratory for Solid State Chemistry & Inorganic Membranes, Department of Materials Science and Engineering, University of Science and Technology of China, Hefei, Anhui 230026, PR China
[b] Anhui Key Laboratory of low temperature co-fired materials, Department of Chemistry, Huainan Normal University, Huainan, Anhui 232001, PR China

ARTICLE INFO

Article history:
Received 27 August 2010
Received in revised form 9 September 2010
Accepted 20 September 2010
Available online 1 October 2010

Keywords:
$(Pr_{0.5}Nd_{0.5})_{0.7}Ca_{0.3}CrO_{3-\delta}$
$Sm_{0.2}Ce_{0.8}O_{1.9}$
Interconnect materials
Sintering ability
Stability

ABSTRACT

$(Pr_{0.5}Nd_{0.5})_{0.7}Ca_{0.3}CrO_{3-\delta}$ (PNCC) interconnect materials are stable in SOFC operating conditions. To improve the sintering ability and electrical conductivity of PNCC, a composite of PNCC/SDC interconnect materials was synthesized by a sol–gel auto-ignition process. The XRD results indicate that PNCC is chemically stable against reaction with SDC at high temperatures. Additionally, SDC-doped PNCC has enhanced sintering activity and electrical conductivity compared to PNCC alone. For 5 wt.% SDC, the relative density of the sample was 95.8% after sintering at 1400 °C, and the electrical conductivity of the sample reached 59.6 S cm^{-1} in air and 4.48 S cm^{-1} in H_2 at 650 °C. Both of these values are higher than those of pure PNCC. The average thermal expansion coefficient of the samples is close to that of other components of SOFCs. Our results indicate that PNCC/SDC composites are promising intermediate materials for IT-SOFCs.

1. Introduction

In recent years, solid oxide fuel cells (SOFCs) have emerged as one of the most important power generation technologies because of their ability to provide high energy conversion efficiency with extremely low pollution [1–4]. The two main components of SOFCs are the cell and the interconnector. The interconnect material connects the anode of one cell to the cathode of the next cell in an electrical series. Up to now, most of the studies concerned with SOFCs have focused on the preparation and the properties of the electrolytes, cathodes and anodes. However, one of the disadvantages of SOFCs is a low voltage output, which limits their commercial application. To raise the voltage output, multiple single cells are electrically connected into stacks via interconnects, which provide the conductive path for electrical current to pass between the electrodes and the external circuit. Currently, determining the best interconnect material is a major challenge in SOFC development. The interconnect material must have good electrical conductivity as well as be stable in both oxidizing and reducing environments, have thermal expansion coefficients (TEC) that are close to those of the other cell components, and have low permeability to oxygen and hydrogen [5–7].

Lanthanum-doped chromite ($LaCrO_3$)-based perovskite phases (ABO_3) are the most reliable candidates as interconnects for SOFCs owing to their thermal and chemical stability as well as their relatively high electrical conductivity in both reducing and oxidizing atmospheres [8–10]. However, Koc et al. [11] reported that a solid solution forms between the $LaCrO_3$ and the $LaMnO_3$ on the interface between the cathode and the interconnector. Furthermore, at high temperatures (>1300 °C), the reaction between $LaCrO_3$ and NiO/YSZ results in the production of a $La_2Zr_2O_7$ phase [12]; this production prohibits the application of $LaCrO_3$ systems. Thus, the substitution of La on A sites is a better choice for co-fired YSZ-based SOFCs. Recently, Wang et al. [13] reported that Ca/Zn-doped $YCrO_3$ as interconnect materials could improve the stability and the sintering ability. Hirota et al. [14] and Shen et al. [15] also reported that Ca-doped $NdCrO_3$ is a promising candidate as an interconnect material in SOFCs.

Little attention has been given to Ca-doped $PrCrO_3$ [16] because its poor sinterability and instability in a reducing atmosphere have limited its application at intermediate temperatures. Recently, $La_{0.7}Ca_{0.3}CrO_3$ and doped CeO_2 composites have also been considered as interconnect materials in SOFCs in the case of negligible oxygen ion conduction. To search for stable and easily sintered interconnect materials for co-fired YSZ-based SOFCs, $(Pr_{0.5}Nd_{0.5})_{0.7}Ca_{0.3}CrO_3$ (PNCC)/$Sm_{0.2}Ce_{0.8}O_{1.9}$ (SDC) composite oxides were prepared by a microwave-assisted auto-ignition process and employed as a new interconnect material. In this work, the sintering activities, crystalline phase structure, electrical conduc-

* Corresponding author. Tel.: +86 551 3606249; fax: +86 551 3607627.
E-mail address: xqliu@ustc.edu.cn (X. Liu).

0378-7753/$ – see front matter © 2010 Elsevier B.V. All rights reserved.
doi:10.1016/j.jpowsour.2010.09.073

tivity and thermal expansion coefficient of PNCC/SDC were studied. The chemical compatibility of PNCC with the NiO–YSZ anode and the $(Pr_{0.5}Nd_{0.5})_{0.7}Sr_{0.3}MnO_3$ (PNSM) cathode was also investigated.

2. Experimental

The fine powders of $(Pr_{0.5}Nd_{0.5})_{0.7}Ca_{0.3}CrO_3$ were synthesized by a microwave-assisted auto-ignition process. The starting materials, $Pr(NO_3)_3{\cdot}6H_2O$(AR), $Nd(NO_3)_3{\cdot}6H_2O$(AR), $Ca(NO_3)_2{\cdot}4H_2O$(AR), and $Cr(NO_3)_3{\cdot}9H_2O$(AR), were dissolved in deionized water at concentrations of ca. 1 mol L^{-1}, and then the molarity was determined accurately by titration with EDTA. For each powder preparation, stoichiometric amounts of nitrate solutions were mixed in an evaporating pot, and then the mixture was added to citric acid (AR) with two times the total amount of nitrates. The mixture was heated using a microwave heating system until the whole solution was converted to a gel. The wet gel was further heated to remove the solvents and became a dry gel. Combustion of the dry gel was carried out at 700 °C, and the resulting powder was calcined for 2 h to obtain the highly reactive fine powders.

$Sm_{0.2}Ce_{0.8}O_{1.9}$ powders were prepared by the auto-ignition method. Stoichiometric amounts of $Sm(NO_3)_3{\cdot}6H_2O$(AR) and $Ce(NO_3)_3{\cdot}6H_2O$(AR) were dissolved in deionized water with 2 mol of citric acid. The mixture was heated using a microwave heating system until the whole solution was converted to a gel. The wet gel was further heated to remove the solvents, resulting in a dry gel. Next, the dry gel was combusted at 700 °C and then calcined for 2 h to obtain the highly reactive fine powders.

The composite powders of PNCC + x wt.% SDC (x = 0, 3, 5 and 7) were mixed by agate-mortar and then pressed into disc-shaped pellets and rectangular bars under 220 MPa using a uniaxial load. The prepared green specimens were sintered in air at 1400 °C for 5 h. The heating rate was maintained at 1 °C min^{-1} before 500 °C and was then increased to 2 °C min^{-1} between 500 °C and 1400 °C.

The phase formations of the sintered specimens were identified using a Dandong Fangyuan X-ray diffractometer (DX-2000) with a Cu Kα radiation source, and the diffraction angle range was (2θ) 20–70°. The densities of the sintered disc-shaped pellets were measured according to the Archimedes principle. The surfaces of the sintered specimens were observed using a scanning electron microscope (SEM, Model KYKY EM 3200). The electrical conductivities of the ceramics were measured in the temperature range of 450–800 °C using a standard DC four-probe technique on an H.P. multimeter (Model 34401). The thermal expansion coefficients were measured from 25 to 1000 °C on disc-shaped pellets using a dilatometer (DIL 402C) at a heating rate of 5 °C min^{-1}.

3. Results and discussion

3.1. XRD phase structure analysis

The XRD patterns of SDC and PNCC/SDC sintered at 1400 °C for 5 h are shown in Fig. 1. The XRD pattern of SDC exhibits a single phase with a fluorite structure. The PNCC specimens all showed a strong intensity for the orthorhombic perovskite phase. The stability of PNCC against reaction with SDC was indicated by the presence of two groups of diffraction peaks in the diffraction patterns. Additionally, the SDC peaks gradually increased as the x value increased, further indicating that there was no reaction between SDC and PNCC.

Because the interconnect materials connect the anode of one cell to the cathode of the next cell in electrical series, XRD analysis was performed on PNCC/NiO–YSZ and PNCC/PNSM pellets after sintering. The XRD patterns of PNCC/NiO–YSZ and PNCC/PSM pellets are shown in Fig. 2. Two groups of diffraction peaks are shown

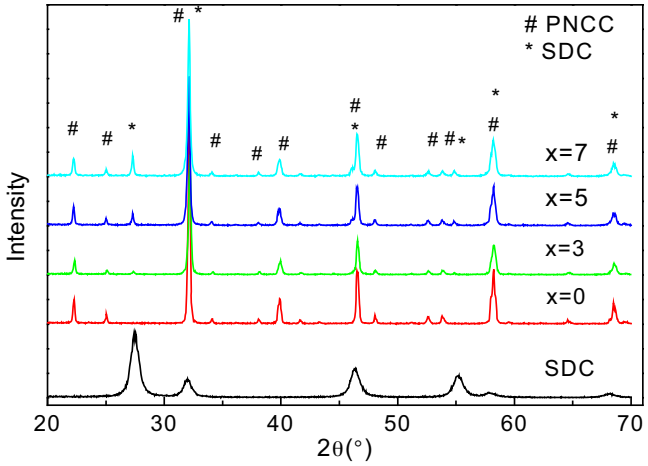

Fig. 1. XRD patterns of PNCC + x wt.% SDC and SDC.

in the diffraction patterns, indicating that PNCC did not react with the NiO–YSZ anode or the PNSM cathode materials at the co-firing temperature (1400 °C).

3.2. Sinterability and SEM analysis

The influence of SDC content in PNCC on the relative density of sintering specimens is shown in Fig. 3. When x was increased from 0 to 3, the relative density of the samples increased sharply from 72% to 94.6%. Upon further increase of x to 7, the relative densities remained approximately at 97%, indicating that the smaller amount of SDC can effectively enhance the sintering ability of the PCC material.

SEM images of the fracture surface morphology of the ceramics for the selected sintering conditions are shown in Fig. 4(a)–(d). As shown in Fig. 4(a), the sample for x = 0 still exists in the first-step of the sintering processes [17]. In Fig. 4(b), the grain structure is compact, and clear grain boundaries can be observed with an average grain size of 2–3 μm. In the same sintering conditions, the grain structure is already quite dense for the specimens of x from 3 to 7 (Fig. 4(c) and (d)). The grains are relatively close and uniform, and grain boundaries are clearly visible with an average grain size about 3–6 μm. These microstructure characteristics indicate that the samples were densely sintered.

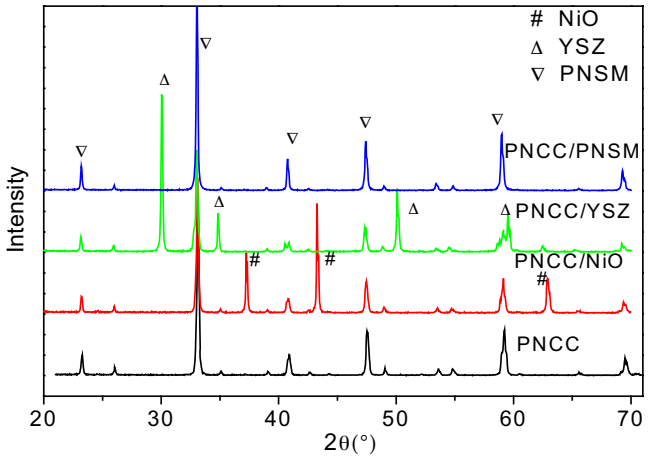

Fig. 2. XRD patterns of the mixtures of NiO–YSZ, PNSM and PNCC after sintering at 1400 °C for 5 h.

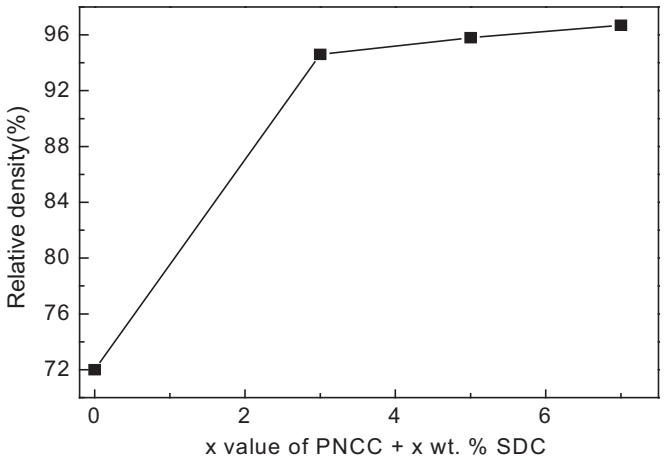

Fig. 3. Relative density of PNCC + *x* wt.% SDC sintered in air at 1400 °C for 5 h.

3.3. Electrical conductivity

Fig. 5(a) shows the temperature dependence of the electrical conductivity of the samples with different *x* content in air. The electrical conductivity of the samples abruptly increased from 16.6 S cm^{-1} to a maximum of 59.6 S cm^{-1} at 650 °C when *x* increased from 0 to 5, respectively. In contrast, the electrical conductivity decreased when *x* was increased from 5 to 7 and dropped to 22.2 S cm^{-1} at *x* = 7. The increase in the electrical conductivity is related to the addition of SDC, which results in the samples having a higher density compared to pure PNCC. Thus, a value of 1 S cm^{-1} is an acceptable minimum electrical conductivity for useful interconnects in SOFCs [18].

The plots of ln(σT) against reciprocal absolute temperature 1/T are illustrated in Fig. 5(b). All plots presented are linear, indicating that the mechanism of conduction can be explained by the small polaron theory [19]. The conductivity data were fitted to the Arrhenius relation for thermally activated conduction:

$$\ln(\sigma T) = \sigma_0 - \frac{E_a}{kT} \quad (1)$$

where E_a is the activation energy for conduction, T is the absolute temperature, k is the Boltzmann constant and σ_0 is the pre-exponential factor. The activation energies of the samples ranged from 13 to 23 kJ mol^{-1}.

Fig. 6 shows the temperature dependence of electrical conductivity of the samples with different *x* content in H_2. The samples of PNCC had relatively low density; as a result, the PNCC sample had low strength and was easy broken at high temperatures in pure H_2. Thus, the electrical conductivity of the PNCC sample was unable to be measured. However, the incorporation of a small amount of SDC can effectively enhance the strength and stability of the PNCC material in H_2. As shown in Fig. 6(a), the electrical conductivities of the samples in pure H_2 were influenced by the amount of SDC. The electrical conductivities increased from 3.01 S cm^{-1} to a maximum of 4.48 S cm^{-1} at 650 °C, with *x* increasing from 3 to 5, respectively. In contrast, the electrical conductivity decreased when *x* was continually increased from 5 to 7, dropping to 3.4 S cm^{-1} at *x* = 7. The

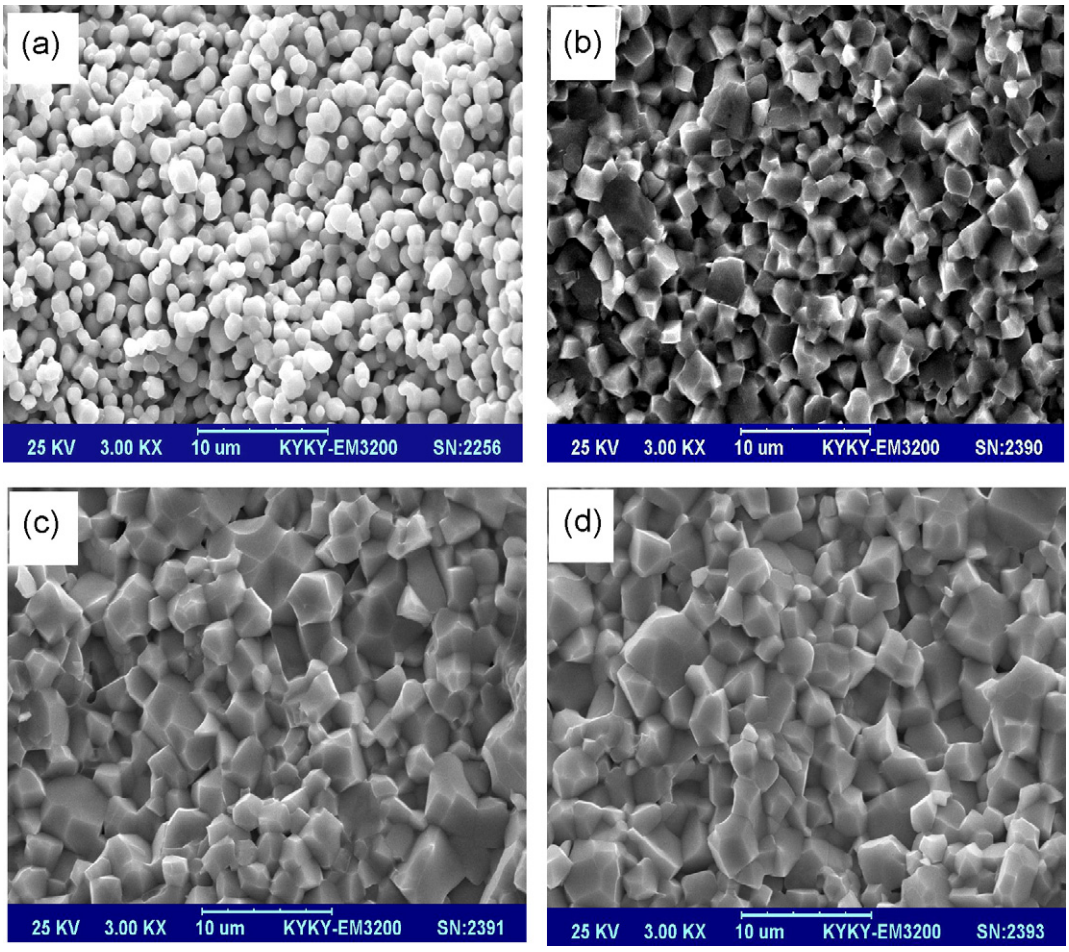

Fig. 4. SEM of PNCC + *x* wt.% SDC sintered in air at 1400 °C for 5 h: (a) *x* = 0; (b) *x* = 3; (c) *x* = 5; (d) *x* = 7.

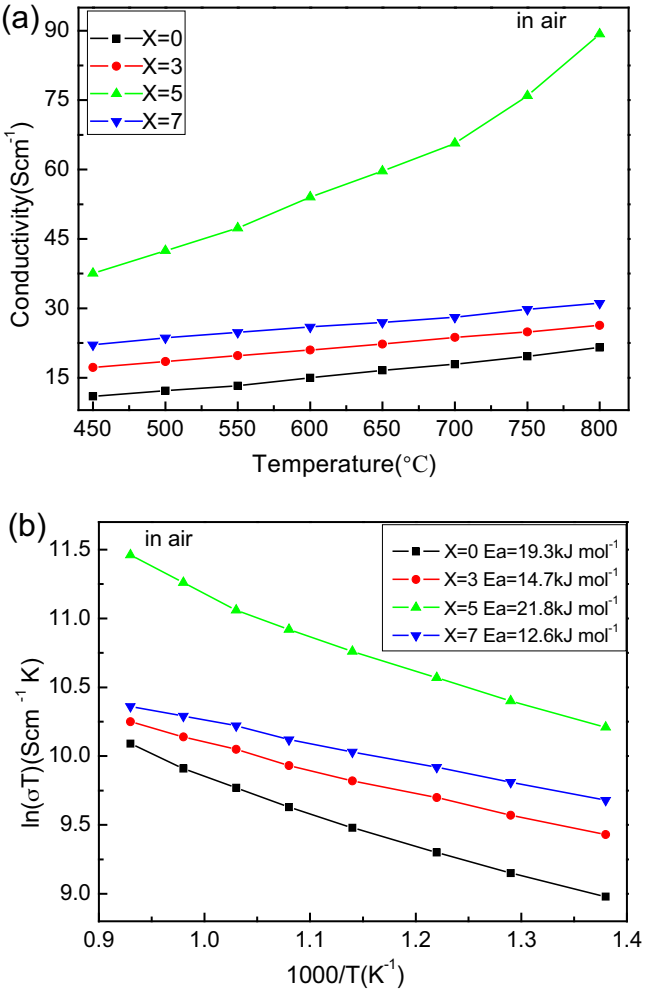

Fig. 5. (a) Electrical conductivity of PNCC + *x* wt.% SDC in air at different temperatures; (b) Arrhenius plots of the conductivities for PNCC + *x* wt.% SDC in air.

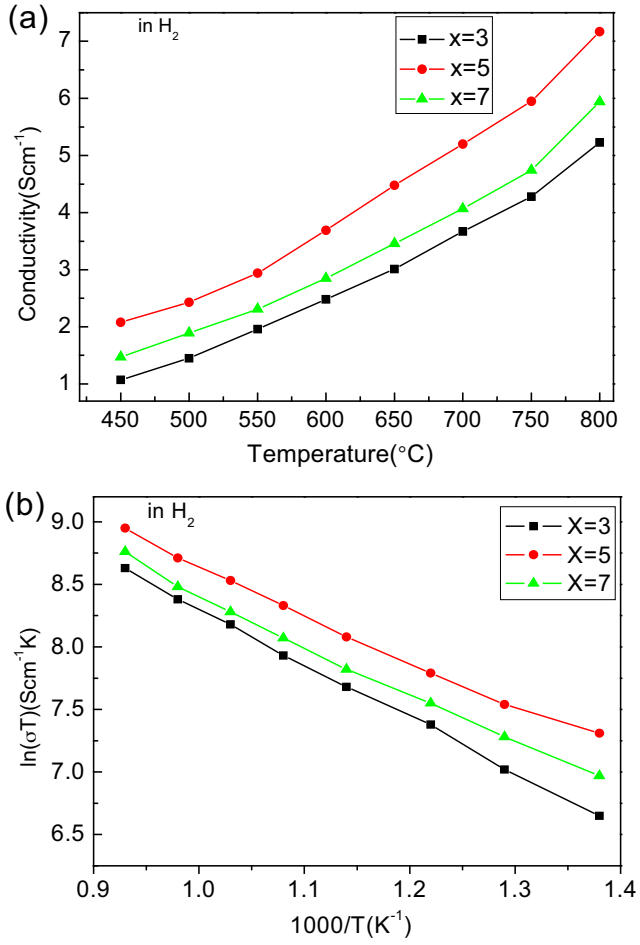

Fig. 6. (a) Electrical conductivity of PNCC + *x* wt.% SDC in H_2 at different temperatures; (b) Arrhenius plots of the conductivities for PNCC + *x* wt.% SDC in H_2.

increase of the electrical conductivity was related to the addition of SDC and increased sample density. Although the electrical conductivity in H_2 was not higher than in air, it was still about 4-times higher than 1 S cm^{-1}, which is the minimum acceptable electrical conductivity for useful interconnects in SOFCs [18]. Higher sample conductivity will further decrease the ohmic loss in IT-SOFCs stacks caused by interconnect material. These materials were also stable in a reducing atmosphere and are therefore suitable for use as interconnect material for IT-SOFCs.

In pure H_2, the plots of $\ln(\sigma T)$ against reciprocal absolute temperature $1/T$ were illustrated in Fig. 6(b). Not all plots were linear. Doped $PrCrO_3$ has been recognized as an orthorhombic perovskite $GdFeO_3$-type conductor [16]. In a high oxygen activity environment, the negatively charged Ca'_{Pr} is electrically compensated by a Cr^{3+} to Cr^{6+} transition to maintain electrical neutrality. The neutrality condition is described as

$$3[Ca'_{Pr}] = [Cr^{\bullet\bullet\bullet}_{Cr}] \quad (2)$$

where [] indicates concentration and $Cr^{\bullet\bullet\bullet}_{Cr}$ indicates Cr^{6+} in the Cr^{3+} site.

When $x \leq 5$, the electrical conductivity increased to the maximum. This increase may have been resulted from an increase in density of the composite materials. However, in the case of $x > 5$, the electrical conductivity decreased. Based on the SDC conduction mechanism, this result can be described according to the equation

$$Sm_2O_3 \xrightarrow{CeO_2} 2Sm'_{Ce} + V^{\bullet\bullet}_O + 3O^{\times}_O \quad (3)$$

In reducing conditions, such as in pure H_2, the lattice oxygen ($O^{\times}_O$) transforms into a doubly charged oxygen vacancies ($V^{\bullet\bullet}_O$), the oxygen vacancies ($V^{\bullet\bullet}_O$) are formed at the expense of losing the charge carriers ($Cr^{\bullet\bullet\bullet}_{Cr}$). That is the reason why the electrical conductivity ability of the material decreased so sharply from air to pure H_2. The balance between the defect species and the surrounding atmosphere can be described as

$$3O^{\times}_O + 2Cr^{\bullet\bullet\bullet}_{Cr} \leftrightarrow \frac{3}{2}O_2 + 3V^{\bullet\bullet}_O + 2Cr^{\times}_{Cr} \quad (4)$$

where $Cr^{\times}_{Cr}$ represents Cr^{3+} in the Cr-site, $V^{\bullet\bullet}_O$ is the oxygen vacancy.

When the environment changes from oxidizing to reducing, the concentration of oxygen vacancies in the samples increases, which is likely due to the reduction of Cr^{6+} to Cr^{3+} and SDC according to Eq. (3) and (4). As a result, the electrical conductivity would significantly decrease in pure H_2. Thus, the electrical conductivity of the composite materials decreased sharply from in air to pure H_2. As shown in Fig. 6(a), the electrical conductivities increased when $x \leq 5$. However, the conductivity of samples decreased when x was further increased to 7, which could be explained by the influence of SDC ($x > 5$)

Thus, the electrical conductivity of the samples is dependent on two different mechanisms. In an oxygen atmosphere such as that in air, the conductivity is attributed to the Cr^{3+} to Cr^{6+} transition via an electronic compensation mechanism. In a reducing atmosphere

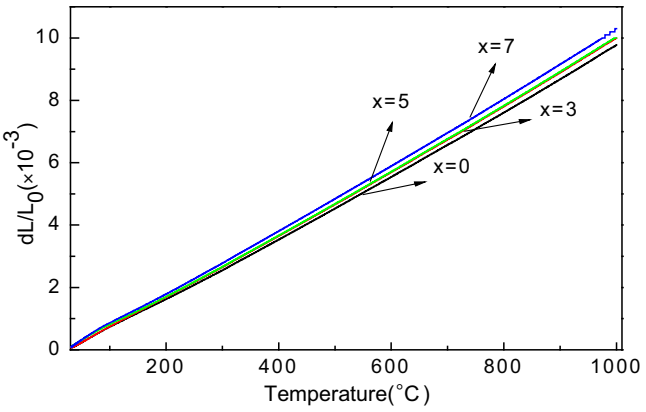

Fig. 7. Thermal expansion of the PNCC + *x* wt.% SDC samples.

such as pure H_2, the conductivity is due to the oxygen vacancy via the ionic compensation mechanism.

3.4. Thermal expansion coefficient

The thermal expansion coefficient (TEC) of interconnects for SOFCs must be close to other cell components to minimize thermal stresses. The TECs of a series of PNCC + *x* wt.% SDC sintered at 1400 °C in air for 5 h are shown in Fig. 7. When *x* increased from 0 to 7, the average linear TEC values of the ceramics increased from $10.1 \times 10^{-6}\,K^{-1}$ to a maximum of $10.5 \times 10^{-6}\,K^{-1}$. Thus, small amounts of SDC had little impact on the TEC of $Pr(Ca)CrO_3$. The TEC of the all samples were close to that of other components of SOFCs, such as the yttria-stabilized zirconia (YSZ) electrolyte (10.5×10^{-6}), the Sr-substituted $PrMnO_3$ cathode (11.1×10^{-6}) and the Ni–YSZ anode (10.8×10^{-6}). Therefore, it will be possible to minimize the thermal stress during the repeated thermal cycles of SOFC stack.

4. Conclusions

The fine powders of PNCC and SDC were synthesized by a sol–gel auto-ignition process. The composite powders of PNCC + *x* wt.% SDC (*x* = 0, 3, 5 and 7) were mixed by agate-mortar. The results indicate that small amounts of SDC doped into PNCC can improve the sintering ability. When *x* is increased from 0 to 5, the relative density of the samples increases sharply from 72% to 95.8%, respectively. The electrical conductivity of the samples abruptly increases from 16.6 S cm^{-1} to 59.6 S cm^{-1} at 650 °C in air. The average thermal expansion coefficient of all samples is $(10.1–10.5) \times 10^{-6}\,K^{-1}$, which is close to that of the other components. These results indicate that the composite PNCC/SDC are a good choice for interconnect materials in IT-SOFCs.

Acknowledgements

The authors acknowledge the support of this research by China Natural Science Foundation on contract No. 50572099 and Scientific and Technological Projects of Huainan under contract No. 2010A03203.

References

[1] H. Ullmann, N. Trofimenko, F. Tietz, et al., Solid State Ionics 138 (2000) 79–90.
[2] S.P. Simner, J.F. Bonnett, N.L. Canfield, et al., J. Powder Sources 113 (2003) 1–10.
[3] H.J. Huang, J.W. Moon, S. Lee, et al., J. Powder Sources 145 (2005) 243–248.
[4] K. Singh, S.A. Acharya, S.S. Bhoga, Solid State Ionics 13 (2007) 429–434.
[5] N.Q. Minh, T. Takahashi, Science and Technology of Ceramic Fuel Cells, Elsevier, Amsterdam, 1995, 165.
[6] S.C. Singhal, K. Kendall, High Temperature Solid Oxide Fuel Cells, Elsevier, Kidlington, 2003, p. 173.
[7] W.Z. Zhu, S.C. Deevi, Mater. Sci. Eng. A 348 (2003) 227–243.
[8] J.W. Fergus, Solid State Ionics 171 (2004) 1–15.
[9] X.L. Zhou, F.J. Deng, M.X. Zhu, et al., J. Power Sources 164 (2007) 293–299.
[10] K. Oikawa, T. Kamiyama, T. Hashimoto, et al., J. Solid State Chem. 154 (2000) 524–529.
[11] R. Koc, H.U. Anderson, J. Mater. Sci. 27 (1992) 5477–5482.
[12] T. Yamamoto, H. Itoh, M. Mori, et al., J. Power Sources 61 (1996) 219.
[13] S.L. Wang, B. Lin, Y.C. Dong, et al., J. Power Sources 61 (2009) 219.
[14] K. Hirota, Y. Kunifusa, M. Yoshinaka, O. Yamaguchi, Mater. Res. Bull. 37 (2002) 2335–2344.
[15] Y. Shen, M. Liu, T. He, S.P. Jiang, J. Power Sources 195 (2010) 977–983.
[16] X.M. Liu, W. Su, Z. Lu, Mater. Chem. Phys. 82 (2003) 327–330.
[17] S.J. Guo, Theory of Powder Sintering Procedure, Metallurgy Industry Press, Beijing, 1998.
[18] N.Q. Minh, C.R. Horne, F.S. Liu, et al., Proceedings of the 25th Intersociety Energy Conversion Engineering Conference, vol. 13, American Institute of Chemical Engineers, New York, 1990, p. 256.
[19] W.J. Weber, C.W. Griffin, V.L. Bates, J. Am. Ceram. Soc. 70 (1987) 265–270.